Workflow Efficiency of High-Density Left Atrial Mapping: A Real-World Benchmark Across Four Multipolar Catheter Designs

Alexandru Gabriel Bejinariu, Nora Augustin, Maximilian Spieker, Carsten auf der Heiden, Stephan Angendohr, David Glöckner, Daniel Oehler, Xenia Xenitidou, Malte Kelm, Obaida Rana

Article - Version of Record

Suggested Citation:
Bejinariu, A. G., Augustin, N., Spieker, M., auf der Heiden, C., Angendohr, S., Glöckner, D., Oehler, D., Xenitidou, X., Kelm, M., & Rana, O. (2026). Workflow Efficiency of High-Density Left Atrial Mapping: A Real-World Benchmark Across Four Multipolar Catheter Designs. Applied Sciences, 16(9), Article 4291.
https://doi.org/10.3390/app16094291

applied sciences

Article

Workflow Efficiency of High-Density Left Atrial Mapping: A Real-World Benchmark Across Four Multipolar Catheter Designs

Alexandru Gabriel Bejinariu [1,*], Nora Augustin [1], Maximilian Spieker [1], Carsten auf der Heiden [1], Stephan Angendohr [1], David Glöckner [1], Daniel Oehler [1], Xenia Xenitidou [1], Malte Kelm [1,2] and Obaida Rana [1]

[1] Division of Cardiology, Pulmonology and Vascular Medicine, Medical Faculty, Heinrich-Heine University, 40225 Düsseldorf, Germany; obaida.rana@med.uni-duesseldorf.de (O.R.)

[2] Cardiovascular Research Institute Düsseldorf (CARID), Medical Faculty, Heinrich-Heine University, 40225 Düsseldorf, Germany

* Correspondence: alexandru-gabriel.bejinariu@med.uni-duesseldorf.de

Abstract

Background: Three-dimensional (3D) mapping of the left atrium (LA) using multipolar high-density (HD) catheters plays a central role in contemporary LA ablation procedures, as accurate and efficient acquisition of anatomical and electrophysiological information is essential. This study benchmarks workflow efficiency during acquisition of a predefined complete HD LA map across four widely used multipolar HD catheter designs. The analysis focuses on efficiency metrics and does not aim to assess mapping quality, arrhythmia interpretation accuracy, or clinical outcomes. **Methods**: We analyzed 182 consecutive patients from an ongoing cohort undergoing LA procedures, including pulmonary vein isolation and complex LA ablations, using 3D mapping in accordance with current guideline recommendations. Four multipolar HD catheters were applied according to the respective 3D mapping systems: a basket catheter (Orion, Rhythmia), a grid catheter (HD Grid, EnSite X), a penta-spline catheter (PentaRay, Carto 3), and an octa-spline catheter (OctaRay, Carto 3). For each procedure, the time required for acquisition of a complete 3D LA map and the number of acquired points were systematically recorded. LA HD mapping speed was calculated by relating LA volume to the time required for complete map acquisition. **Results**: The study population had a mean age of 69 years, with a median CHA_2DS_2-VASc score of 3, indicating a cohort with a moderate thromboembolic risk profile. The median LA volume index (LAVI) was 34 mL/m^2. Patients were distributed across four HD catheter groups, comprising 44 patients in the basket group, 29 in the grid group, 23 in the penta-spline group, and 86 in the octa-spline group. LA mapping speed differed significantly among the groups, with values of 3 mL/min in the basket group, 2.5 mL/min in the grid group, 3.1 mL/min in the penta-spline group, and the highest mapping speed observed in the octa-spline group at 5.9 mL/min. **Conclusions**: The octa-spline catheter was associated with a significantly higher LA mapping speed compared with other widely used HD catheters.

Keywords: 3D mapping; mapping speed; high-density multipolar catheters

Academic Editor: Piotr Gas

Received: 14 February 2026
Revised: 18 April 2026
Accepted: 21 April 2026
Published: 28 April 2026

1. Introduction

Left atrial (LA) ablations are the cornerstone of interventional therapy in the management of atrial fibrillation (AF) and complex atrial tachycardias (AT). With increasing complexity of the procedure, multipolar high-density mapping catheters (HDMCs) play a central role, as gaining anatomical, bipolar and activation data during short amounts of time becomes indispensable.

Bipolar data have been proven to be of crucial importance, as they serve useful for the guidance of ablation in patients with persistent AF with improved outcomes in a pulmonary vein isolation (PVI) together with a tailored ablation strategy directed at atrial low-voltage regions, as demonstrated by the ERASE-AF trial [1]. Further strategies in ablation of AF/AT such as the addition of vein of Marshall ethanol infusion to PVI [2] and ablation of deceleration zones after isochronal late activation mapping [3] also imply multiple LA maps, increasing LA dwell and procedure time – important predictors of cerebral lesions [4].

Furthermore, the use of HDMCs in patients with paroxysmal or persistent AF undergoing PVI using a 3D mapping system is an elegant alternative for creating anatomical maps for point-by-point mapping with the ablation catheter accompanied by the angiography of the pulmonary veins for defining the ostia. Also, HDMCs improve the detection of gaps during a "de novo" PVI as compared to circular mapping catheters [5].

With increasing availability of HDMCs, there is a clear clinical need for the rapid acquisition of high-density LA 3D maps.

While electroanatomic mapping primarily serves accurate substrate characterization and, when applicable, robust interpretation of AT mechanisms, modern LA ablation workflows frequently require repeated mapping and remapping. In this setting, workflow efficiency—i.e., the time and signal acquisition required to obtain a predefined complete LA map—represents a relevant and measurable technology performance dimension. Therefore, we benchmarked four widely used multipolar HD catheter designs with respect to efficiency metrics during acquisition of a standardized complete LA map: a basket catheter (Orion, Rhythmia), a grid catheter (Advisor HD Grid, EnSite X) and two multi-spline catheters—a penta-spline catheter (Pentaray, Carto3) and an octa-spline catheter (OctaRay, Carto3)—see Figure 1.

A. Basket catheter

B. Grid catheter

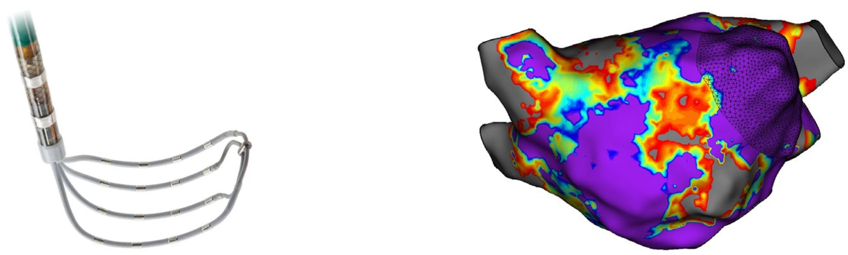

Figure 1. *Cont.*

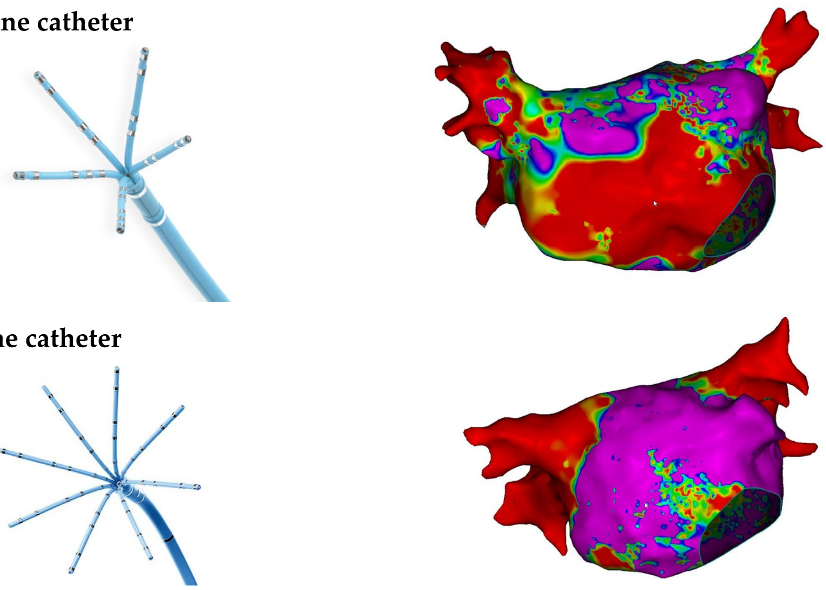

Figure 1. Overview of high-density mapping catheters and representative left atrial maps.

In this context, the proposed metric should be understood as an operational measure of workflow efficiency rather than as a surrogate for mapping quality or clinical benefit.

2. Materials and Methods

2.1. Ethical Approval

The study protocol received approval from the local ethics committee of Heinrich Heine University Düsseldorf (Study Number 2019-555_4) and was conducted in accordance with the principles outlined in the Declaration of Helsinki. Prior to inclusion in the study, all participants provided written informed consent after receiving detailed information about the nature and purpose of the investigation.

2.2. Patient Population

We retrospectively studied consecutive patients undergoing left atrial procedures at our institution from June 2022 until May 2023 using a 3D mapping system. Patients with paroxysmal atrial fibrillation (AF), persistent AF and atrial tachycardia (AT) refractory to antiarrhythmic treatment (class I and III antiarrhythmics) were considered eligible if they were older than 18 years of age and provided informed consent before inclusion. Patients were excluded if they had a contraindication to oral anticoagulation, left atrial thrombus on preprocedural transesophageal echocardiography (TEE) or valvular AF. The procedures were indicated in accordance with the most recent guideline recommendations from the European Society for Cardiology (ESC) [6]. With increasing availability of HDMCs there is a clear clinical need for the rapid acquisition of high-density LA 3D maps.

The primary endpoint of the study was the mapping speed of the HDMCs, defined as the LA volume measured by echocardiography divided by the time needed to create the complete LA map. The secondary endpoint was the overall procedure duration, fluoroscopy time and fluoroscopy dose.

Comorbidities, medications, and epidemiological data were recorded and analyzed.

2.3. Procedural Details

All ablation procedures were conducted under intravenous sedation. Sedative management consisted of midazolam and propofol, with additional piritramide administered when necessary. Throughout the procedure, continuous monitoring of heart rate, oxygen saturation, and non-invasive blood pressure was performed in accordance with institutional standards. For the ablation procedures we used the US4ABL workflow [7]. TEE was routinely used to exclude LA thrombus and to support transseptal puncture. Femoral vascular access was guided by ultrasound (US). After completion of the procedure, transthoracic echocardiography (TTE) was performed to rule out pericardial effusion, in accordance with our previously established protocol.

Oral anticoagulation was managed according to a minimally interrupted strategy. Anticoagulant therapy was withheld on the evening prior to the procedure and routinely resumed on the evening following the intervention after exclusion of pericardial effusion by echocardiographic assessment. This approach was chosen to balance procedural safety with the need to minimize thromboembolic risk during the periprocedural period [8].

All procedures were performed by two experienced electrophysiologists, each of whom had performed more than 1000 ablation procedures using each respective 3D mapping system prior to the study period. The predefined procedural endpoints were determined by the specific type of LA intervention performed and were adapted to the underlying arrhythmia substrate and procedural objective:

(1) In procedures performed for pulmonary vein isolation (PVI), a wide-area circumferential ablation strategy was applied around the pulmonary vein (PV) antra using an ablation index-guided approach. Lesion delivery was guided by predefined ablation index targets to ensure consistent lesion quality and transmurality. The procedural endpoint of PVI was defined as complete electrical isolation of all PVs, confirmed by the absence of PV signals recorded using either a circular mapping catheter or a HDMC following completion of the ablation.

(2) In procedures performed for LA tachycardias, detailed electroanatomical mapping was carried out using a HDMC to delineate the underlying arrhythmia mechanism and critical conduction pathways. Based on the individual activation and voltage characteristics identified during mapping, lesion sets were selected at the operator's discretion and tailored to the specific tachycardia substrate. The procedural endpoint was defined as non-inducibility of the clinical AT following completion of the ablation. All deployed linear lesion sets were systematically evaluated for bidirectional conduction block to confirm their electrophysiological effectiveness. All AT cases included in this study were macroreentrant; no focal AT was included.

We used four HDMCs, which could be grouped into three categories, according to their designs:

- A 64-electrode basket catheter: Orion, in combination with the Rhythmia 3D mapping system (Figure 1A);
- A 16-electrode grid catheter: Advisory HD Grid, in combination with the En Site X 3D mapping system (Figure 1B);
- Two multi-spline catheters: 22-electrode penta-spline (Pentaray) and 48-electrode octa-spline (Octaray), in combination with the CARTO3 3D mapping system (Figure 1C and 1D, respectively).

Catheter use followed a stable institutional workflow throughout the study period and was not selectively adapted to specific case types.

2.4. Assessment of the Mapping Speed

We defined the mapping speed as the LA volume divided by the time needed to create the complete LA map:

$$\text{Mapping speed} = \frac{\text{Left atrial volume [mL]}}{\text{Mapping time [min]}}$$

After the transseptal puncture with a steerable sheath (Agilis NxT, Abbott), the HDMC was introduced in the LA and a complete LA map (bipolar map and activation map) was created using the HDMC and the steerable sheath by thoroughly covering every segment of the LA (posterior wall, pulmonary veins, inferior wall, lateral wall, anterior wall and septum), ensuring the best possible contact. Importantly, mapping was not restricted to pulmonary vein anatomy, even in procedures performed for PVI, but aimed at comprehensive LA coverage in all cases. The falsely annotated electrograms (EGMs) were eliminated.

A complete LA map was defined by systematic anatomical coverage of all predefined LA segments rather than by a predefined minimum number of acquired EGMs. Mapping was continued until all segments were adequately represented and no relevant anatomical gaps were present. Platform-specific mapping algorithms and fill thresholds were applied according to the recommended settings of each 3D mapping system. Because EGM/point counting depends on platform-specific acquisition and annotation settings, absolute EGM counts were reported descriptively, whereas between-group comparisons focused on EGM acquisition speed and volume-normalized LA mapping speed. During AT, activation maps were considered complete when a stable and interpretable activation pattern covering the entire LA was achieved. Mapping was performed in sinus rhythm (including after cardioversion in patients with persistent AF) or during AT, reflecting the standardized mapping conditions used for workflow benchmarking in this cohort.

Mapping was performed under deep sedation, which was routinely achieved due to TEE conducted prior to LA mapping. Procedural interruptions due to sedation instability were therefore uncommon. In cases where AT degenerated into AF during mapping, electrical cardioversion was performed and LA mapping was subsequently repeated. In these cases, mapping time was defined as the uninterrupted mapping period required to acquire a complete LA map after rhythm stabilization. Repeated catheter repositioning to ensure optimal contact and complete LA coverage was considered an integral part of the mapping process and was included in the recorded mapping time.

Furthermore, the LA volume was assessed during the postprocedural TTE (for effusion rule-out) using a Vivid T8 machine (GE Healthcare, Chicago, IL, USA) according to the guidelines of the American Society of Echocardiography [9]. The bi-plane method of disks (modified Simpson's rule; apical four-chamber and two-chamber views) was employed to calculate the LA volumes.

2.5. Statistics

Statistical analyses were performed using SPSS version 28 (SPSS Inc., Chicago, IL, USA) and Prism 10. Continuous data are presented as mean ± standard deviation or as the median with interquartile range (IQR), whereas categorical variables are reported as absolute numbers and percentages. Data distribution was evaluated using the Shapiro–Wilk test. Comparisons of continuous variables were conducted using the Mann–Whitney U test. Relationships between categorical or discrete variables were analyzed using the Pearson χ^2 test or Fisher's exact test, as appropriate.

3. Results

A total of 182 consecutive patients were included in the final analysis. The baseline demographic and clinical characteristics of the study cohort are provided in Table 1, allowing for a comprehensive overview of patient profiles across the different catheter groups.

https://doi.org/10.3390/app16094291

Table 1. Baseline characteristics.

	All Patients n = 182	Basket n = 44	Grid n = 29	Penta-Spline n = 23	Octa-Spline n = 86	*p* Value
Age, years	69 (62–77)	68 (60–77)	70 (63–77)	70 (65–79)	69 (61–77)	0.70
Male gender —n (%)	98 (54)	22 (50)	16 (55)	8 (35)	38 (44)	0.47
BMI—kg/m^2 (IQR)	27 (25–32)	29 (25–34)	27 (25–30)	27 (24–32)	27 (25–32)	0.62
CHA_2DS_2-VASc score (IQR)	3 (2–4)	3 (2–4)	3 (2–4)	3 (2–4)	3 (2–4)	0.97
Hypertension —n (%)	127 (70)	29 (66)	17 (59)	19 (82)	62 (72)	0.26
Diabetes mellitus—n (%)	18 (10)	6 (14)	2 (7)	1 (4)	9 (10)	0.61
History of stroke—n (%)	18 (10)	6 (14)	3 (10)	1 (4)	8 (9)	0.67
History of MI —n (%)	18 (10)	3 (7)	3 (10)	3 (13)	9 (10)	0.86
Heart failure —n (%)	52 (28)	12 (27)	9 (31)	8 (35)	23 (27)	0.87
OSA—n (%)	27 (15)	7 (16)	3 (10)	5 (22)	12 (14)	0.70
Echocardiography						
LA volume—ml (IQR)	68 (46–91)	71 (49–97)	63 (43–97)	58 (40–81)	75 (47–95)	0.26
LAVI—ml/m^2 (IQR)	34 (24–46)	35 (27–46)	32 (23–46)	30 (21–39)	37 (25–48)	0.26
LV EF—% (IQR)	59 (56–62)	59 (56–62)	58 (55–62)	61 (58–63)	59 (56–62)	0.29
Type of arrhythmia						
Paroxysmal AF	91 (50)	17 (39)	18 (62)	12 (52)	44 (51)	0.25
Persistent AF	70 (38)	22 (50)	9 (31)	7 (30)	32 (37)	0.28
Atrial tachycardia	22 (12)	5 (11)	2 (7)	5 (21)	10 (12)	0.42

IQR interquartile range, *BMI* body mass index, *MI* myocardial infarction, *AF* atrial fibrillation, *LV* left ventricle, *LA* left atrium, *OSA* obstructive sleep apnea, *LAVI* left atrial volume index, and *LV EF* left ventricular ejection fraction.

The study population had a mean age of 69 years, reflecting an elderly cohort with relevant comorbidity burden. The median CHA_2DS_2-VASc score was 3, indicating a high thromboembolic risk, and the median LA volume index (LAVI) measured 34 mL/m^2.

The study cohort was stratified into four groups according to the type of HD catheter used, with each group comprising a predefined number of patients based on the mapping system and catheter design applied during the procedure: 44 (basket group), 29 (grid group), 23 (penta-spline group) and 86 (octa-spline group), respectively. The baseline characteristics did not differ among the four groups. Likewise, arrhythmia categories were similarly distributed across groups, arguing against preferential use of specific catheter types in fundamentally different clinical settings.

Procedural characteristics are summarized in Table 2. Overall procedure duration differed significantly between the study groups, primarily driven by the shorter procedure times observed in the octa-spline group compared with the grid group. In contrast, the radiation dose area product did not show significant differences across the four groups.

Table 2. Procedural characteristics.

	Basket n = 44	Grid n = 29	Penta-Spline n = 23	Octa-Spline n = 86	*p* Value
Procedural duration—min (IQR)	138 (113–171)	146 (118–172)	132 (110–172)	123 (106–151)	0.02
Fluoroscopy time—min (IQR)	13 (8–17)	16 (11–22)	8 (7–10)	10 (7–14)	<0.01
DAP—cGy*cm^2 (IQR)	497 (330–771)	549 (370–778)	383 (270–600)	433 (302–677)	0.12

IQR interquartile range and *DAP* dose area product.

No major periprocedural complications were documented in the study cohort; minor access-site events were not systematically recorded.

The map characteristics differed significantly among the groups (Table 3). The absolute number of points (acquired EGMs) was the highest in the basket group (mean of 9133 EGMs) and the mapping time was the highest in the octa-spline group (11 min). Absolute EGM counts varied across systems, consistent with platform-specific acquisition and annotation algorithms; therefore, comparative interpretation primarily relied on EGM acquisition speed and volume-normalized mapping speed.

Table 3. Map characteristics.

	Basket n = 44	Grid n = 29	Penta-Spline n = 23	Octa-Spline n = 86	*p* Value
Mapping system	Rhythmia	EnSite X	Carto 3	Carto 3	N/A
Algorithms	Version 5.0	Version 2.0.1 OT, absolute dV/dt max	Version 7.2 TPI, maximum density, point filtering 5 mm, fill threshold 5 mm	Version 7.2 TPI, maximum density, point filtering 5 mm, fill threshold 5 mm	N/A
Acquired EGMs	9133 (6605–12,974)	3306 (2682–4351)	1923 (1158–2915)	5177 (3668–6700)	<0.001
Mapping duration—min (IQR)	24 (20–30)	21 (18–25)	18 (17–23)	11 (10–14)	<0.001
Mapping speed—mL/min (IQR)	3 (2–3.97)	2.5 (1.8–4.4)	3.1 (2.3–4.1)	5.9 (4.3–8.4)	<0.001
EGM acquisition speed—points/min (IQR)	390 (255–724)	144 (111–234)	91 (62–152)	472 (301–670)	<0.001

OT omnipolar technology, *TPI* tissue proximity indicator, *IQR* interquartile range, *EGM* electrogram, and *N/A* not applicable.

A significant difference in LA mapping speed was observed among the four HD catheter groups. The octa-spline catheter achieved the highest mapping speed, with a median value of 5.9 mL/min, indicating substantially faster acquisition of complete LA maps compared with the other catheter designs. In contrast, mapping speed was markedly lower in the penta-spline group, with a median of 3.1 mL/min, and was comparable in the basket group and the grid group, with median values of 3 mL/min and 2.5 mL/min, respectively.

Pairwise statistical analyses confirmed that LA mapping speed obtained with the octa-spline catheter was significantly higher than that achieved with each of the other HD catheters investigated in this study. No statistically significant differences in mapping speed were detected between the penta-spline, basket, and grid catheter groups, suggesting broadly comparable performance among these three designs with respect to this parameter. These findings are illustrated in Figure 2.

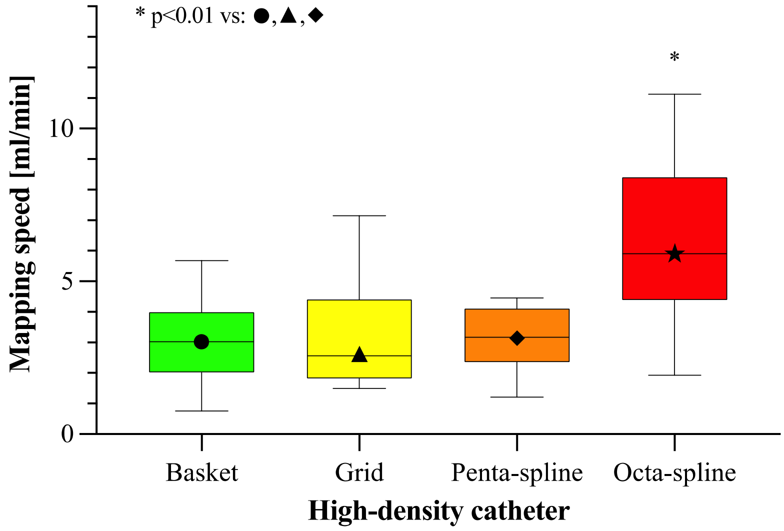

Figure 2. Left atrial mapping speed of the four high-density mapping catheters.

Furthermore, the speed of the EGM acquisition also differed significantly among the four groups, with the highest values for the octa-spline and basket catheters (median of 472 and 389 points/mL, respectively), as shown in Figure 3.

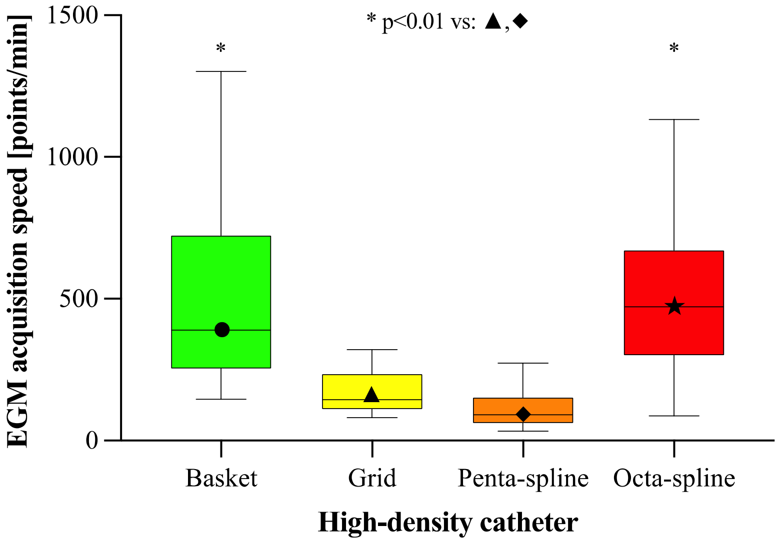

Figure 3. Acquisition speed of electrograms of the four high-density mapping catheters. *EGM* electrogram.

4. Discussion

Our findings should be interpreted as a real-world benchmark of workflow efficiency during acquisition of a predefined complete HD LA map using contemporary multipolar catheter designs. We intentionally focused on efficiency metrics rather than clinical outcomes, because technology benchmarking requires an operationally defined and comparable mapping task across platforms. Accordingly, the results do not imply superiority in arrhythmia interpretation or mapping quality but quantify differences in mapping throughput within routine clinical workflows.

We compared four of the available and most used multipolar HDMCs (basket, grid, penta-spline and octa-spline) in terms of mapping speed and EGM acquisition speed. We defined the mapping speed as the volume of the LA measured by TTE divided by the number of minutes needed to create the complete LA map, and the EGM acquisition speed as the number of EGMs (points) acquired per minute.

The clinical relevance of this metric lies primarily in procedural workflow rather than in a proven direct impact on patient outcomes. In complex LA procedures requiring repeated mapping and remapping, a higher volume-normalized mapping speed may reduce mapping-related procedural burden; however, whether this translates into improved safety or long-term clinical outcomes is beyond the scope of the present study.

The main findings are as follows: (1) the mapping speed was significantly higher for the octa-spline catheter compared to each of the other catheters and (2) the EGM acquisition speed was significantly higher for the basket and the octa-spline HDMCs.

Systematic benchmarking of HD mapping efficiency has only rarely been reported, likely because mapping objectives and workflows differ substantially across clinical scenarios. By operationalizing a standardized complete LA mapping task and using a volume-normalized efficiency metric, our study enables a pragmatic real-world comparison across contemporary catheter designs.

To the best of our knowledge, this is the first study to define a measure for the LA mapping speed. Moreover, we systematically analyzed and compared the performance of four different HDMCs using this new measure technique. The octa-spline catheter not only proved to be the fastest catheter but also was as fast as the basket catheter in terms of EGM acquisition speed.

The available studies in the literature report the number of points and the mapping time with a wide variety of clinical questions, without considering the LA volume measured by a standardized method such as TTE [10–13]. We believe that this is the main strength of our study—the implementation of a new unit of measurement for the mapping speed of HDMCs.

Moreover, our data (mapping time and number of EGMs) are in line with those of the published studies: for instance, the number of points gathered with the octa-spline catheter was roughly four times higher than the number of points gathered with the penta-spline catheter, exactly as previously reported [14].

The ablation of persistent AF and post-PVI LA tachycardias requires complex lesion sets and long procedure times, including mapping and remapping of both atria [1,2,15,16]. Therefore, maintaining an LA dwell time as low as possible to avoid thromboembolic complications is essential [17], particularly in complex LA procedures requiring repeated mapping. In this context, the octa-spline catheter demonstrated a significantly higher LA mapping speed and EGM acquisition speed compared with the other investigated HDMCs, indicating higher workflow efficiency under the conditions of the present study.

Outcome data were not part of the present analysis; therefore, no conclusions could be drawn regarding potential effects on arrhythmia recurrence or other clinical outcomes. Likewise, the present findings should not be interpreted as evidence of superior mapping quality or overall procedural superiority.

Our study has several limitations. Although a standardized HDMC-based mapping workflow was applied and LA mapping was not restricted to pulmonary vein anatomy, it cannot be fully excluded that mapping performed in the context of PVI may, in routine clinical practice, be less detailed than mapping performed for complex AT. This potential difference in mapping behavior represents an inherent limitation of comparative studies conducted in real-world settings. Secondly, the groups are unbalanced in terms of the number of patients, and the larger size of the octa-spline group may theoretically have increased operator familiarity with this catheter over time. However, all procedures were performed by highly experienced operators familiar with all three 3D mapping systems, making a relevant influence of operator-dependent factors or learning curve effects unlikely. Thirdly, the LA mapping was done under sinus rhythm or during AT, not under pacing with a fixed cycle length. Mapping was performed in sinus rhythm to avoid the induction of AF in patients with persistent AF who required cardioversion immediately prior to mapping. Finally, this was a single-center study performed by two operators; although a standardized workflow was applied throughout, external reproducibility across additional centers and operators should be confirmed in future multicenter studies.

In addition, echocardiographic parameters derived from speckle tracking echocardiography, such as LA reservoir strain, were not included in the present analysis. Impairment of LA reservoir strain has been shown to identify patients with AF at higher risk of LA appendage dysfunction, spontaneous echocardiographic contrast, or thrombus formation [18,19]. Integration of speckle tracking echocardiography-derived parameters may therefore provide complementary functional insights beyond anatomical mapping alone and should be considered in future studies.

5. Conclusions

This study shows that the octa-spline catheter was associated with higher LA mapping speed and higher EGM acquisition speed than the other investigated HDMCs. These findings support the use of volume-normalized LA mapping speed as a pragmatic metric of workflow efficiency during the acquisition of a complete LA map. Whether these efficiency differences translate into improved procedural safety or clinical outcomes remains to be determined in future prospective studies.

Author Contributions: A.G.B. and N.A. prepared the manuscript with all text tables, figures and references and were responsible for data acquisition, statistical analyses and interpretation of data. M.S., C.a.d.H., S.A., D.G., D.O. and X.X. were responsible for data acquisition. A.G.B., O.R. and M.K. were involved in the concept and design of this study as the principal investigators and were responsible for statistical analyses and interpretation of data. All authors were responsible for inclusion of patients and were involved in the critical manuscript revision for important intellectual content. All authors have read and agreed to the published version of the manuscript.

Funding: A publication grant from Biosense Webster (Irvine, CA, USA) supported the preparation of this manuscript (BWI-PG-11). The sponsor had no role in the study design, data collection, analysis, interpretation, or writing of the manuscript.

Institutional Review Board Statement: This study was conducted in accordance with the Declaration of Helsinki and approved by the Institutional Ethics Committee at the Faculty of Medicine of Heinrich Heine University Düsseldorf.

Informed Consent Statement: Informed consent was obtained from all subjects involved in the study.

Data Availability Statement: Raw data were generated at the University Hospital in Düsseldorf, Germany. The data that support the findings of this study are available from the principal investigator on reasonable request.

Conflicts of Interest: The authors have nothing to declare related to the current work.

References

1. Huo, Y.; Gaspar, T.; Schönbauer, R.; Wójcik, M.; Fiedler, L.; Roithinger, F.X.; Martinek, M.; Pürerfellner, H.; Kirstein, B.; Richter, U.; et al. Low-Voltage Myocardium-Guided Ablation Trial of Persistent Atrial Fibrillation. *NEJM Evid.* **2022**, *1*, EVIDoa2200141. [CrossRef] [PubMed]
2. Valderrábano, M.; Peterson, L.E.; Swarup, V.; Schurmann, P.A.; Makkar, A.; Doshi, R.N.; DeLurgio, D.; Athill, C.A.; Ellenbogen, K.A.; Natale, A.; et al. Effect of Catheter Ablation with Vein of Marshall Ethanol Infusion vs Catheter Ablation Alone on Persistent Atrial Fibrillation: The VENUS Randomized Clinical Trial. *JAMA* **2020**, *324*, 1620–1628. [CrossRef] [PubMed]

3. Kuo, M.-J.; Ton, A.N.-K.; Lo, L.-W.; Lin, Y.-J.; Chang, S.-L.; Hu, Y.-F.; Chung, F.-P.; Tuan, T.-C.; Chao, T.-F.; Liao, J.-N.; et al. Abnormal Conduction Zone Detected by Isochronal Late Activation Mapping Accurately Identifies the Potential Atrial Substrate and Predicts the Atrial Fibrillation Ablation Outcome After Pulmonary Vein Isolation. *Circ. Arrhythm. Electrophysiol.* **2023**, *16*, e011149. [CrossRef] [PubMed]
4. Boga, M.; Suhai, F.I.; Orbán, G.; Salló, Z.; Nagy, K.V.; Szegedi, L.; Jokkel, Z.; Csőre, J.; Osztheimer, I.; Perge, P.; et al. Incidence and Predictors of Stroke and Silent Cerebral Embolism Following Very High-Power Short-Duration Atrial Fibrillation Ablation. *Europace* **2023**, *25*, euad327. [CrossRef] [PubMed]
5. Vandenberk, B.; Quinn, F.R.; Barmby, J.; Wilton, S.B.; Kuriachan, V. High-Density Mapping Improves Detection of Conduction Gaps after Pulmonary Vein Isolation Ablation with a Circular Mapping Catheter. *J. Interv. Card. Electrophysiol.* **2023**, *66*, 1401–1410. [CrossRef] [PubMed]
6. Van Gelder, I.C.; Rienstra, M.; Bunting, K.V.; Casado-Arroyo, R.; Caso, V.; Crijns, H.J.G.M.; De Potter, T.J.R.; Dwight, J.; Guasti, L.; Hanke, T.; et al. 2024 ESC Guidelines for the Management of Atrial Fibrillation Developed in Collaboration with the European Association for Cardio-Thoracic Surgery (EACTS): Developed by the Task Force for the Management of Atrial Fibrillation of the European Society of Cardiology (ESC), with the Special Contribution of the European Heart Rhythm Association (EHRA) of the ESC. Endorsed by the European Stroke Organisation (ESO). *Eur. Heart J.* **2024**, *45*, 3314–3414. [CrossRef] [PubMed]
7. Bejinariu, A.G.; Augustin, N.; Spieker, M.; auf der Heiden, C.; Angendohr, S.; Höckmann, M.; Clasen, L.; Hartl, S.; Makimoto, H.; Busch, L.; et al. The US4ABL Strategy: A Systematic Ultrasound-Guided Approach for Left Atrial and Ventricular Ablation Procedures. *J. Clin. Med.* **2025**, *14*, 103. [CrossRef] [PubMed]
8. Bejinariu, A.G.; Makimoto, H.; Wakili, R.; Mathew, S.; Kosiuk, J.; Linz, D.; Steinfurt, J.; Dechering, D.G.; Meyer, C.; Veltmann, C.; et al. One-Year Course of Periprocedural Anticoagulation in Atrial Fibrillation Ablation: Results of a German Nationwide Survey. *Cardiology* **2020**, *145*, 676–681. [CrossRef] [PubMed]
9. Lang, R.M.; Badano, L.P.; Mor-Avi, V.; Afilalo, J.; Armstrong, A.; Ernande, L.; Flachskampf, F.A.; Foster, E.; Goldstein, S.A.; Kuznetsova, T.; et al. Recommendations for Cardiac Chamber Quantification by Echocardiography in Adults: An Update from the American Society of Echocardiography and the European Association of Cardiovascular Imaging. *J. Am. Soc. Echocardiogr.* **2015**, *28*, 233–271. [CrossRef] [PubMed]
10. Kaseno, K.; Hasegawa, K.; Miyazaki, S.; Mukai, M.; Aoyama, D.; Nodera, M.; Hirano, K.; Otake, M.; Nomura, R.; Miyahara, K.; et al. Discrepancy Between CARTO and Rhythmia Maps for Defining the Left Atrial Low-Voltage Areas in Atrial Fibrillation Ablation. *Heart Vessel.* **2021**, *36*, 1027–1034. [CrossRef] [PubMed]
11. Miyazaki, S.; Hasegawa, K.; Yamao, K.; Mukai, M.; Aoyama, D.; Sekihara, T.; Nodera, M.; Eguchi, T.; Iesaka, Y.; Tada, H. High-Resolution Mapping and Ablation of Atrial Tachycardias Involving the Lateral Left Atrium. *J. Am. Heart Assoc.* **2021**, *10*, e022384. [CrossRef] [PubMed]
12. Saito, J.; Yamashita, K.; Numajiri, T.; Gibo, Y.; Usumoto, S.; Narui, S.; Fujioka, T.; Asukai, Y.; Igawa, W.; Ono, M.; et al. Grid-Mapping Catheters versus PentaRay Catheters for Left Atrial Mapping on Ensite Precision Mapping System. *J. Cardiovasc. Electrophysiol.* **2022**, *33*, 1405–1411. [CrossRef]
13. Starek, Z.; Di Cori, A.; Betts, T.R.; Clerici, G.; Gras, D.; Lyan, E.; Della Bella, P.; Li, J.; Hack, B.; Zitella Verbick, L.; et al. Baseline Left Atrial Low-Voltage Area Predicts Recurrence after Pulmonary Vein Isolation: WAVE-MAP AF Results. *EP Eur.* **2023**, *25*, euad194. [CrossRef] [PubMed]
14. Masuda, M.; Matsuda, Y.; Uematsu, H.; Asai, M.; Okamoto, S.; Ishihara, T.; Nanto, K.; Tsujimura, T.; Hata, Y.; Higashino, N.; et al. Comparison of Voltage Maps Using OCTARAY Catheter and PENTARAY Catheter. *Pacing Clin. Electrophysiol.* **2024**, *47*, 28–35. [CrossRef] [PubMed]
15. Takagi, T.; Derval, N.; Duchateau, J.; Chauvel, R.; Tixier, R.; Marchand, H.; Bouyer, B.; André, C.; Kamakura, T.; Krisai, P.; et al. Gaps after Linear Ablation of Persistent Atrial Fibrillation (Marshall-PLAN): Clinical Implication. *Heart Rhythm* **2023**, *20*, 14–21. [CrossRef] [PubMed]
16. Deisenhofer, I.; Albenque, J.-P.; Busch, S.; Gitenay, E.; Mountantonakis, S.E.; Roux, A.; Horvilleur, J.; Bakouboula, B.; Oza, S.; Abbey, S.; et al. Artificial Intelligence for Individualized Treatment of Persistent Atrial Fibrillation: A Randomized Controlled Trial. *Nat. Med.* **2025**, *31*, 1286–1293. [CrossRef] [PubMed]
17. Kamioka, M.; Watanabe, T.; Watanabe, H.; Okuyama, T.; Yokota, A.; Komori, T.; Kabutoya, T.; Imai, Y.; Kario, K. High-Power Short-Duration Setting Prevents Changes of Periprocedural Thrombotic Markers and the Onset of Silent Stroke in Patients with Atrial Fibrillation. *Heart Rhythm* O^2 **2024**, *5*, 917–924. [CrossRef] [PubMed]

18. Sonaglioni, A.; Lombardo, M.; Nicolosi, G.L.; Gensini, G.F.; Ambrosio, G. Mechanical Concordance Between Left Atrium and Left Atrial Appendage in Nonvalvular Atrial Fibrillation: Can It Be Exploited to Avoid Transesophageal Echocardiography Prior to Electrical Cardioversion During Covid-19 Pandemic? *Int. J. Cardiovasc. Imaging* **2022**, *38*, 351–362. [CrossRef] [PubMed]
19. Kiliszek, M.; Uziębło-Życzkowska, B.; Krzyżanowski, K.; Jurek, A.; Wierzbowski, R.; Smalc-Stasiak, M.; Krzesiński, P. Value of Left Atrial Strain in Predicting Recurrence after Atrial Fibrillation Ablation. *J. Clin. Med.* **2023**, *12*, 4034. [CrossRef]